Eur Biophys J (2003) 31: 575–585
DOI 10.1007/s00249-002-0253-z

ARTICLE

**Michael Rappolt · Mónica Fernández Vidal
Manfred Kriechbaum · Milos Steinhart
Heinz Amenitsch · Sigrid Bernstorff · Peter Laggner**

Structural, dynamic and mechanical properties of POPC at low cholesterol concentration studied in pressure/temperature space

Received: 4 April 2002 / Accepted: 2 August 2002 / Published online: 25 October 2002

Abstract We have studied the structural, dynamic and mechanical properties of 1-palmitoyl-2-oleoyl-*sn*-glycero-3-phosphatidylcholine (POPC)/cholesterol binary mixtures by small-angle X-ray scattering. Our investigations were concentrated on the biologically most relevant pressure-temperature-cholesterol regime, i.e. the liquid crystalline phase and its phase boundary to the lamellar gel phase within a cholesterol concentration up to 25 mol%. From the dependence of the transition pressure we derived a value of 19 kJ/mol for the transition enthalpy ΔH_m of POPC in excess water. With increasing cholesterol concentration, ΔH_m drops to about 7 kJ/mol at 20 mol% cholesterol. Time-resolved pressure-scan (p-scan) and temperature-jump (T-jump) experiments reveal that at low cholesterol content (< 5–8 mol%) the fluidity and also the bilayer compressibility increase remarkably. In contrast, at concentrations between 5 and 25 mol% cholesterol the bilayer becomes again more rigid and the lipid bilayer spacing increases about 2 Å. Theses changes are attributed to the onset of phase separation between liquid disordered and liquid ordered phases. The fluid-fluid miscibility gap for this mono-unsaturated lecithin species is strongly enlarged compared with saturated lecithins.

Keywords Cholesterol · Phosphatidylcholine · Pressure scan · Temperature jump · Phase separation

M. Rappolt · M.F. Vidal · M. Kriechbaum · H. Amenitsch
P. Laggner (✉)
Institute of Biophysics and X-Ray Structure Research,
Austrian Academy of Sciences,
Schmiedlstrasse 6, 8042 Graz, Austria
E-mail: peter.laggner@oeaw.ac.at
Tel.: +43-316-4120301
Fax: +43-316-4120390

M. Steinhart
Institute of Macromolecular Chemistry,
Academy of Sciences of the Czech Republic,
Prague, Czech Republic

S. Bernstorff
Sincrotrone Trieste, Strada Statale 14, km 163.5,
34012 Basovizza (TS), Italy

Abbreviations *HP-cell*: high pressure cell · *ld*: liquid disordered · *lo*: liquid ordered · *PC*: phosphatidylcholine · *POPC*: 1-palmitoyl-2-oleoyl-*sn*-glycero-3-PC · *SAXS*: small-angle X-ray scattering · *so*: solid ordered · *SOPC*: 1-stearoyl-2-oleoyl-*sn*-glycero-3-PC

Introduction

Cholesterol is an essential and ubiquitous biochemical component in the lipid bilayer of plasma membranes in eukaryotic cells. Its unique amphiphilic property to control both fluidity and order-disorder states in the bilayer has been the subject of intense investigations over the past decades (for reviews, see Vist and Davis 1990; Finegold 1993; Mouritsen and Jørgensen 1994; McMullen and McElhaney 1995). Many different techniques have been used in studying phosphatidylcholine/cholesterol model systems, such as NMR spectroscopy (Thewalt and Bloom 1992; Huster and Gawrisch 2000), electron paramagnetic resonance (Pasenkiewicz-Gierula et al. 1990; Sankaram and Thompson 1991), stationary and time-resolved fluorescence spectroscopy (Almeida et al. 1992; Parasassi et al. 1995; Drake and Burton 1998), small-angle neutron and X-ray scattering (McIntosh et al. 1989; Lemmich et al. 1997; Richter et al. 2001), calorimetry (Mabrey et al. 1978; Davis and Keough 1983; McMullen et al. 1993), theoretical approaches (Ipsen et al. 1987; Cruzeiro-Hansson et al. 1989; Anderson and McConnell 2001) and molecular dynamics as well as Monte-Carlo simulations (Scott 1993; Tu et al. 1998; Nielsen et al. 1999; Chiu et al. 2001; Miao et al. 2002).

In vivo, the relative content of cholesterol is variable and depends on the source of the membrane. It can reach – for instance in cell plasma membranes – up to 50 mol%, whereas it is much less abundant in internal membranes. The lowest concentration is found in the inner mitochondria membranes (Jamieson and Robinson 1977) and in the membranes of the endoplasmic reticulum (< 5 mol%), which, interestingly, is the site of cholesterol biosynthesis (Lange et al. 1999). The most

dominant feature of cholesterol in living cells can be attributed to its function as a fluidity regulator. It is also involved in the regulation of membrane protein interaction and activity (Presti 1985; Yeagle 1993). Briefly summarized, cholesterol affects mechanical and thermodynamic properties of the lipid bilayer with increasing concentration in the following ways: (1) a decrease of the area per lipid molecule in the fluid phase (Ipsen et al. 1990; Smaby et al. 1997; Worthman et al. 1997); (2) a broadening (between 5–25 mol% cholesterol) up to the complete abolition of the cooperative gel to liquid crystalline phase transition (above about 25–30 mol% cholesterol); (3) above 5–8 mol%, cholesterol decouples the conformational order from the crystalline order and, as a consequence, induces the formation of a new liquid ordered phase (Ipsen et al. 1987); (4) cholesterol preferentially interacts with a subset of membrane lipids, and thus can partition lipid bilayers into cholesterol-rich and cholesterol-poor regions (Radhakrishnan and McConnell 1999; Dietrich et al. 2001).

Since only relatively few studies have focused on the very low to low cholesterol concentration regime (Rukmini et al. 2001), we attempted in our present work to study the structural, dynamic and mechanical properties of lecithin/cholesterol systems below 25 mol% cholesterol by means of X-ray scattering together with pressure-scan and temperature-jump techniques, respectively. In contrast to the majority of experimental studies, which have involved dipalmitoyl- or dimyristoyl-phosphatidylcholine (DPPC, DMPC), we have chosen palmitoyl-oleoyl-phosphatidylcholine (POPC) as a model bilayer system, for the following reasons. First, most of the eukaryotic cells of PC/cholesterol mixtures often have a high concentration of unsaturated lipids. To mention but a few, symmetrically and asymmetrically unsaturated phospholipids and cholesterol are found in essential biological membranes such as in the nervous system, postsynaptic membranes, retinal rod outer segment, and sperm heads (Salem 1989). Second, several studies on PC-bilayer systems consisting also of unsaturated chains have led to the conclusion that different chain conformations create a fluid phase microimmiscibility. This may lead to cholesterol-rich and cholesterol-poor microdomains but rich in unsaturated chains, which may in turn be important for the stabilization of specific protein functions in biological membranes (Mitchell and Litman 1998; Brzustowicz et al. 2002). Last, with the choice of POPC as a model membrane, the *p*-*T*-cholesterol phase diagram of interest, with the lamellar gel phase and the liquid crystalline phase, lies in an experimentally easily accessible region.

We focus in this work on the coexistence region of the gel and fluid phase, and on the phase separation regime of the cholesterol/phospholipid bilayers. A variety of detailed experiments have led to a widely accepted temperature/composition phase diagram as shown in Fig. 1 (Ipsen et al. 1987; Thewalt and Bloom 1992; Mateo et al. 1995). The pure gel and fluid phases, respectively, which are often referred to as solid ordered (*so*) and liquid disordered (*ld*), are maintained up the eutectic point at about 5–8 mol% cholesterol, i.e. the freezing point decreases only slightly (from –5 to –7 °C) with increasing amounts of cholesterol and thereafter remains nearly constant. Above 5–8 mol%, cholesterol induces in either phase a new liquid ordered phase (*lo*) which coexists with *so* and *ld* up to 25–30 mol%, beyond which only *lo* exists.

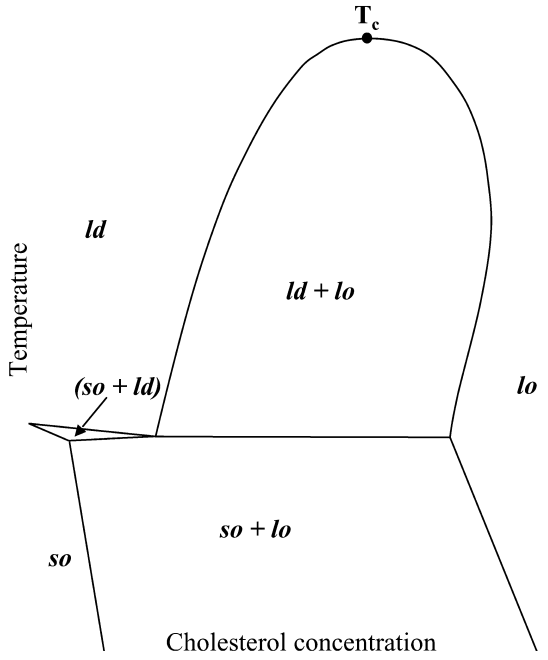

Fig. 1 Schematic phase diagram of PC/cholesterol mixtures as a function of temperature. The phases are characterized as follows: *so*: translationally and configurationally ordered; *ld*: translationally and configurationally disordered; *lo*: translationally disordered and configurationally ordered. T_c marks the critical point

In our present studies, the barotropic phase transition between the fluid and gel phase of POPC/cholesterol was explored in pressure-scan experiments by time-resolved small-angle X-ray scattering (SAXS). The liquid crystalline (fluid) phase has been studied at ambient pressure by static SAXS measurements in a temperature range from 10 to 50 °C, and also in rapid T-jump experiments with millisecond time resolution. The static diffraction patterns obtained under equilibrium conditions were analysed in terms of the modified Caillé theory (Pabst et al. 2000a), and hence the most important structural parameters, i.e. the bilayer spacing and the interbilayer water spacing, could be derived for the *ld* and *ld*/*lo* phase regions. The mechanical properties of the bilayer have been studied by small T-jump perturbations at low temperature, where the bilayer reacts as an over-damped oscillator (Pabst et al. 2000b).

Materials and methods

Sample preparation

1-Palmitoyl-2-oleoyl-*sn*-glycero-3-phosphatidylcholine (POPC) and cholesterol were purchased from Avanti Polar Lipids (Birmingham,

Ala., USA; >99%), and used without further purification. To prepare the samples, suitable quantities of lipid and cholesterol in a range from 1 to 25 mol% were mixed and dissolved in an organic solution of chloroform/methanol (2:1, v/v), which was then left to evaporate under a stream of nitrogen at a temperature between 60 °C and 70 °C, to form a thin lipid film on the bottom of the glass vials. After the last visible traces of solvent had been removed, the samples were kept under vacuum (~1 kPa) at 20 °C, i.e. above the chain-melting temperature (T_m), for about 8 h. The lipid mixtures were then suspended in the amount of deionized water necessary to obtain the desired lipid concentration (20–25 w/w). To ensure complete hydration, the lipid dispersions were incubated for about 4 h at least 10 °C above the main transition temperature. During this period the lipid dispersions were vigorously vortexed. Using this method of liposome preparation, the samples without cholesterol display a narrow, cooperative melting transition during slow p-scans (Winter and Pilgrim 1989). Thin layer chromatography carried out on all samples before and after experimentation showed no sign of degradation.

Small-angle X-ray diffraction

Diffraction patterns were recorded at the SAXS beamline at ELETTRA, Trieste, Italy (Amenitsch et al. 1998; Bernstorff et al. 1998), using a one-dimensional position-sensitive detector (Gabriel, Grenoble, France) covering the corresponding reciprocal s-range ($s = 2\sin\theta/\lambda$, with λ the wavelength and 2θ the scattering angle) of interest from about 1/200 Å^{-1} to 1/12 Å^{-1}. The angular calibration of the detector was performed with silver behenate with a d-spacing of 58.38 Å (Huang et al. 1993) and also with dry rat-tail tendon collagen (d-spacing = 650 Å).

For the high-pressure experiments we have utilized a high-pressure X-ray cell (HPXC) (Pressl et al. 1997), where X-ray scattering experiments can be performed under hydrostatic pressures up to 300 MPa and temperatures between –20 °C and +80 °C. The computer-aided pressure adjustment had a calibrated precision of ±0.5%, and the temperature was computer-controlled to a precision of ±0.05 °C. Pressures up to 200 MPa were produced by a motor-driven, piston-type generator by compressing a fluid of low compressibility (water) and by transmitting it via a high-pressure network into the sample cell (HPXC). The cell had two diamond windows with a thickness of either 0.5 or 0.75 mm with a total transmission of 0.7 at 16 keV photon energy, leaving a free optical path length of 3 mm and allowing scattering to be observed at angles up to 30°. The samples (less than 30 µL) were filled in a capsule of cylindrical shape (length 3 mm, diameter 3 mm) made of aluminium, sealed at both ends with a mylar foil of 100 µm thickness, in order to avoid contamination or dilution with the pressurizing medium water, and inserted into the high-pressure cell. All functions of the experimental setup (temperature, pressure, scan rate) were personal computer controlled and synchronized with the X-ray data acquisition (number of diffraction frames, exposure times). The pressure scans at a given scan rate (from 1 to 4 MPa/s) were performed from 0.1 MPa up to 200 MPa (and back to <5 MPa) at each constant temperature ranging from 5 °C up to 20 °C, taking single diffraction patterns typically every 2 s. This led to a total exposure time of 250 s for a reversible p-scan from 0.1 to 200 MPa and back. For comparison, static measurements with 20 s exposure were also performed.

For the T-jump measurements, the lipid dispersions were kept in a thin-walled 1-mm diameter quartz capillary held in a steel cuvette, which provided good thermal contact to the Peltier heating unit (Anton Paar, Graz, Austria). T-jumps were generated with an erbium-glass infrared laser (Kriechbaum et al. 1990; Rapp and Goody 1991). The laser-pulse energy was set to 0.5 J, resulting in an average T-jump amplitude, ΔT, of 3.3 ± 0.5 °C. The variation of the T-jump amplitude derives mainly from the difficulty in measuring precisely the energy deposited onto the sample, which depends on the precision of measuring the laser-pulse energy (±5%), the estimation of the geometric properties in the experimental setup (~10% error) and the estimation of the absorption in the sample (~10% error); however, the reproducibility of the laser-pulse energy lies within 2%. A time-resolved experiment (one cycle) consisted of a series of 256 time-frames of pattern detection, with the laser (pulse length 2 ms) triggered at the beginning of the 11th frame. The maximum time resolution of the X-ray experiment, i.e. the first frame after the laser shot, was set to 5 ms. The total exposure time of one cycle was 16 s. Each experiment was repeated 10 times, i.e. every diffraction pattern was averaged over 10 cycles.

Data analysis

The raw data of the time-resolved experiments were normalized for the integration time of each time frame, and the background was subtracted. Static powder diffraction data were corrected for the detector efficiency, background scattering from water and the sample cell scattering was then subtracted. The static diffraction patterns at ambient pressure were analysed over the full s-range by the MCG method (for details, see Pabst et al. 2000a), which combines a modified Caillé theory for the structure factor with a form factor of a Gaussian representation of the electron density profile. In brief, the bilayer thickness d_B is expressed as a function of the head group position and its widths:

$$d_B = 2(z_H + \mathrm{fwhm}_H/2) \quad (1)$$

where z_H is the position of the head group with respect to the bilayer center at the methyl terminus, and the size of the head group is estimated by the full width at half maximum (fwhm_H) of the Gaussian, representing the electron density profile in the head group region.

The interbilayer water layer is defined as the difference of the d-spacing minus the bilayer thickness:

$$d_W = d - d_B \quad (2)$$

For the non-static experiments, i.e. the p-scans and the T-jumps, only the first-order Bragg peaks of the recorded diffraction patterns were analysed with standard peak-fitting routines. Here, we used the Lorentzian distribution to model the first-order reflection.

The relaxation kinetics of the lamellar repeat distance d after the T-jump perturbation is given by a double-exponential decay (Laggner et al. 1999):

$$d(t) = d_{eq} - d_a \exp(-t/\tau_a) - d_b \exp(-t/\tau_b) \quad (3)$$

where d_{eq} is the equilibrium d-spacing at the given system temperature before the T-jump, d_a and d_b are relaxation components and τ_a, τ_b the respective relaxation time constants. The relaxation kinetics of the d-spacing can be regarded as a harmonic, one-dimensional overdamped oscillation (Pabst et al. 2000b).

Results

Slow pressure scans

Using the high-pressure X-ray cell (Pressl et al. 1997; Steinhart et al. 1999) we have performed slow, reversible pressure scans (~2.5 MPa/s) at constant temperatures on various POPC/cholesterol dispersions in excess water (75–80% w/w) and monitored the changes in d, the lamellar repeat spacing, by SAXS in real time. Pure POPC in excess water has its chain melting transition at –5 °C, at ambient pressure (Winter and Pilgrim 1989).

In Fig. 2, time-resolved X-ray diffraction patterns are shown for POPC with 1 mol% cholesterol at 20 °C during a p-scan (pressurizing and subsequent depressurizing) in the s-range of the first- and second-order Bragg peaks corresponding to the d-spacing of the

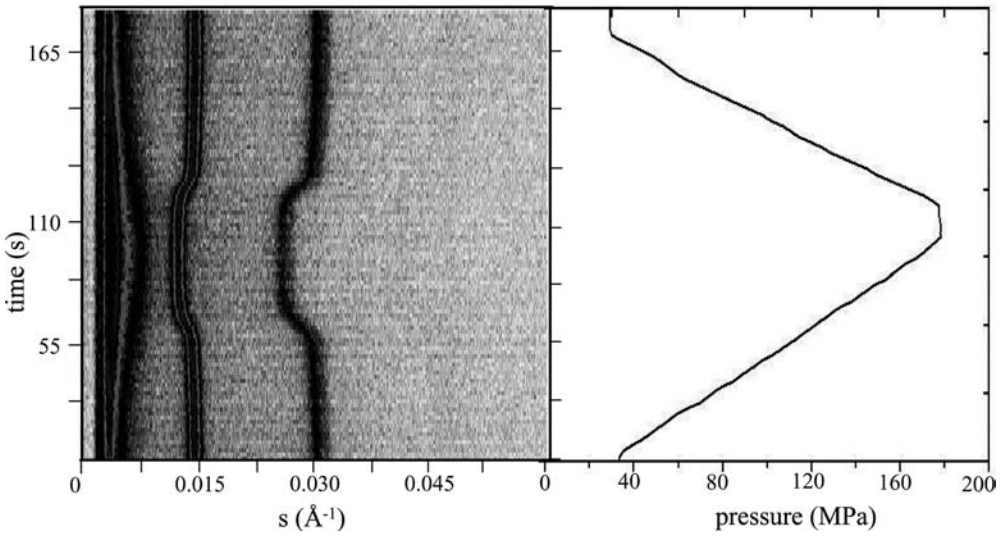

Fig. 2 Main transition of POPC (20 wt%, 1 mol% cholesterol, 20 °C) during a pressurizing and depressurizing scan, respectively. *Left*: time-resolved SAXS patterns (85 frames, each 2 s exposure time) in a contour plot are shown; *right*: for each frame the corresponding pressure value is displayed in a vertical plot

lamellar lattice. The inflection points of the d versus p function correspond to the transition pressure p_m from the liquid crystalline phase to the gel phase and vice versa. In the pressurizing direction, p_m has a value of 150 MPa, and in the depressurizing mode of 100 MPa, respectively. To estimate the "equilibrium" transition pressure p_m, we have taken the mean value of both inflection points.

We have performed such p-scans for POPC with different concentrations of cholesterol (0, 1, 5, 10 and 20 mol%) at different temperatures. The transition pressures p_m were derived for each concentration within a temperature range from 5 to 20 °C. For 0 and 20 mol% cholesterol, respectively, the transition pressure p_m as a function of temperature is shown in Fig. 3A. Increasing the cholesterol concentration, the slopes of dp_m/dT decrease slightly (Fig. 3B). Using the Clapeyron relation $dT_m/dp = T_m \Delta V_m/\Delta H_m$, the enthalpies ΔH_m were estimated for 1–20 mol% cholesterol. For this, the respective volume changes ΔV_m for the POPC/cholesterol mixtures have been approximated by re-scaling the equivalent values for DPPC/cholesterol from density scanning experiments (Melchior et al. 1980). The scaling factor was obtained from the known ratio of ΔV_m(POPC)/ΔV_m(DPPC) for the pure lipids, with ΔV_m(POPC) = 15.5 cm^3/mol (Ichimori et al. 1999). In Fig. 3C, the enthalpy ΔH_m values are shown as a function of the cholesterol concentration. The numerical results from Fig. 3 are summarized in Table 1.

For the pressure dependence of the lamellar d-spacing (at 20 °C) in slow p-scans (compression and decompression), we observed a significant hysteresis effect of the transition pressure p_m with increasing concentration of cholesterol, reaching a maximum at 5 mol% cholesterol (Fig. 4). Pure POPC displays the smallest hysteresis width (18 MPa), and upon increasing the concentration of cholesterol it increases from 56 MPa for 1 mol% to 92 MPa for 5 mol% cholesterol. Beyond this, the width and the shape change significantly owing to the appearance of the *lo* phase. At 10 mol% cholesterol the hysteresis is reduced to 78 MPa, but already at 20 mol% cholesterol concentration the initially sigmoidal shape of the d-spacing versus pressure curves is flattened out, and thus a determination of the hysteresis width is not possible. However, all recorded barotropic transitions are reversible, i.e. the initial d-spacings are always recovered after one loop. The hysteresis loops were repeated up to three times. The pressure hysteresis widths Δp_m, which are reproducible at the same scan rates, are summarized in Fig. 5.

Static and temperature jump studies

At ambient pressure, static diffraction patterns have been recorded between 10 and 50 °C in steps of 5 °C, for cholesterol contents between 0 and 20 mol%. All diffraction patterns were analysed using the MCG method (see Data analysis section), and the most significant parameters, i.e. the d-spacing, the bilayer spacing d_B, and the interbilayer water spacing d_W, are mapped in contour plots in Fig. 6A–C. As indicated by the dashed line in Fig. 6B, the boundary between the *ld* and the *ld*/*lo* phases at about 5 mol% cholesterol can be clearly seen. The averaged bilayer thickness of the *ld*/*lo* phase is by about 2 Å larger than in the pure phase region and also the thinning of the membrane as a function of temperature is less pronounced. Opposite tendencies can be seen in the d_W map (Fig. 6C).

The mechanical properties of the bilayer membrane as a function of cholesterol content have been investigated in T-jumps with a jump amplitude of 3 °C. The relaxation kinetics of the T-jump-induced perturbations have been analysed in terms of the relaxation model presented in the Data analysis section (for details see Pabst et al. 2000b). The starting temperature in every

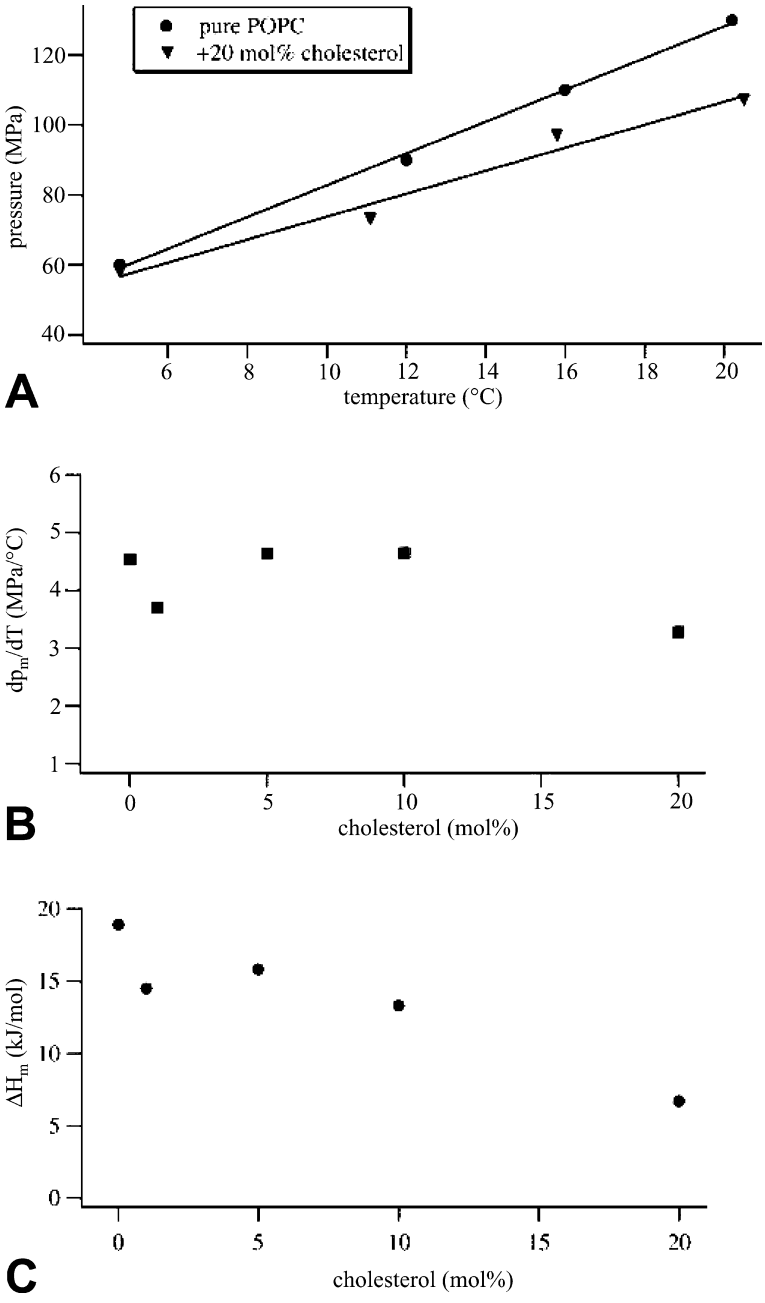

Fig. 3A–C Thermodynamic properties for the main transition of POPC with increasing cholesterol concentrations. **A** Transition pressure p_m as a function of the temperature for pure POPC (20 wt%) and for POPC + 20 mol% cholesterol obtained from pressure scans followed by SAXS. **B** dp_m/dT as a function of different concentrations of cholesterol; p_m represents the "equilibrium transition pressure" (see text). **C** Transition enthalpy ΔH_m as a function of the cholesterol concentration obtained from the experimental dp_m/dT and ΔV values from the literature (compare Table 1)

Table 1 Thermodynamic properties for the main transitions of POPC with increasing cholesterol concentrations

Cholesterol (mol%)	ΔV (cm^3/mol)[a] DPPC	ΔV (cm^3/mol) POPC	dp_m/dT (MPa/°C) POPC	ΔH_m (kJ/mol) POPC
0	26.6	15.5	4.5	18.9
1	22	14.7	3.7	14.5
5	19	12.7	4.6	15.8
10	16	10.7	4.6	13.3
20	11.4	7.6	3.7	6.7

[a]Values taken from Melchior et al. (1980)

experiment was 10 °C. The relaxation components of the over-damped oscillation are given in Table 2.

Figure 7A displays a typical temporal evolution of the lamellar repeat distances during a T-jump experiment. The solid line gives the best fit of the relaxation model in Eq. (3). In Fig. 7B the maximum change of the *d*-spacing as a function of cholesterol content is plotted. Since the water compressibility is by about one order of magnitude lower than that of the lipids, the total thinning of the *d*-spacing, Δd_{max}, can be directly associated with the fluidity of the membrane bilayer alone. Thus, up to 5 mol%, cholesterol enhances the fluidity of the acyl chains, but above this amount a rigidification is induced.

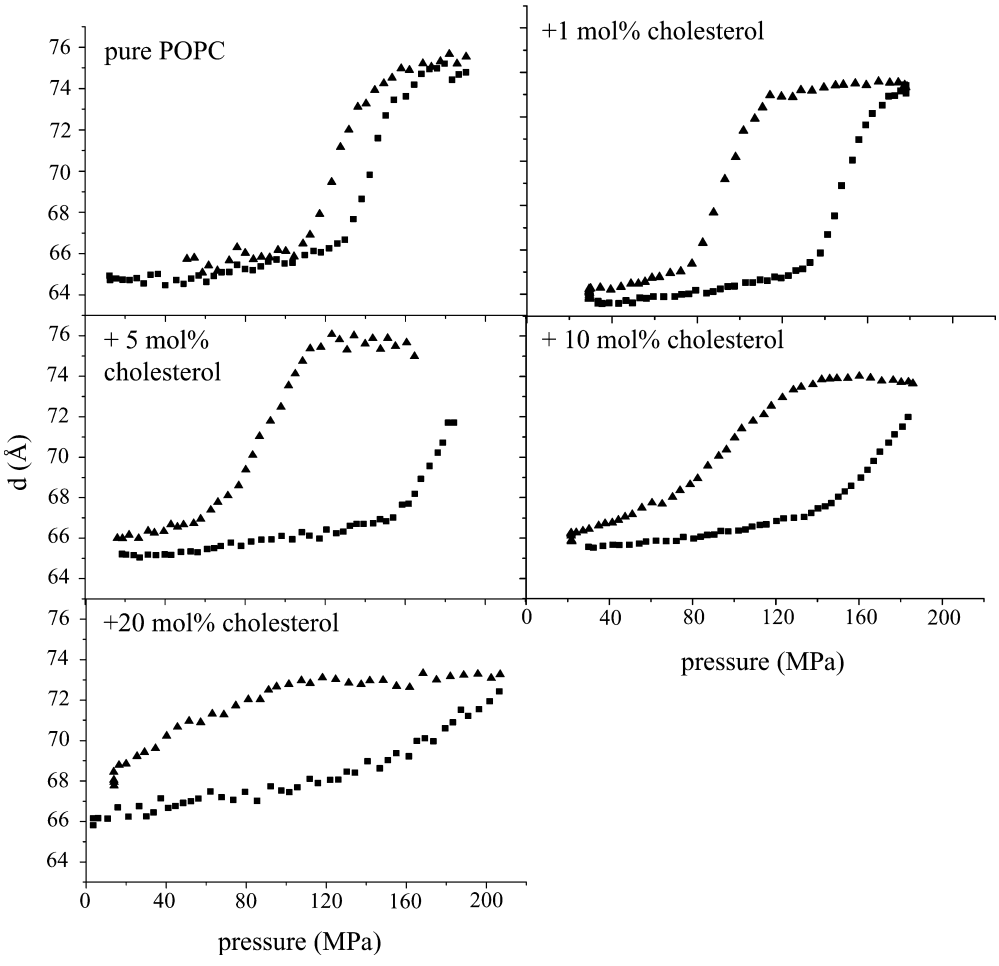

Fig. 4 Lamellar *d*-spacings of POPC as a function of pressure during pressurizing (*squares*) and depressurizing (*triangles*) scans, respectively. All scans were carried out at 20 °C

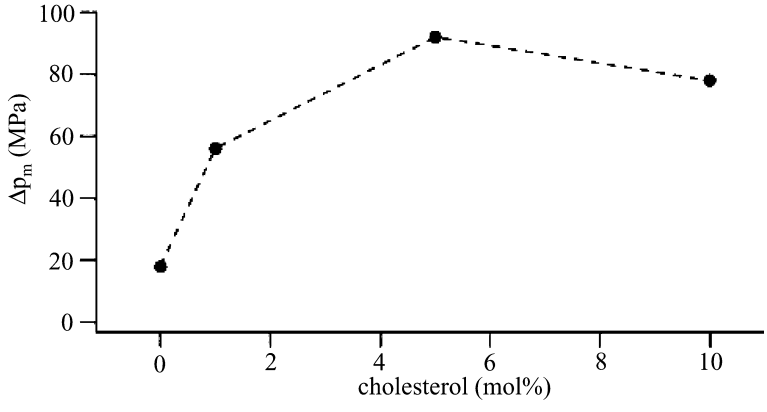

Fig. 5 Barotropic hysteresis width Δp at the main transition of POPC evaluated from the plots in Fig. 4 as a function of cholesterol content

Discussion

Extension of the phase diagram

It is generally believed that the *lo* phase is the biologically relevant phase, e.g. for the organization of the plasma membrane of eukaryotic membranes (Bloch 1965, 1983, 1994). Under conservation of the membrane fluidity, cholesterol can increase the mechanical strength of cells and at the same time also increase their selectivity owing to the reduced membrane permeability (Bloom and Mouritsen 1995). Many studies on model membranes containing low to medium concentrations of cholesterol (5–25 mol%) prove the fluid-fluid miscibility gap, where the cholesterol-rich *lo* phase coexists with the fluid disordered phase, to be one of the most important topics in binary lipid systems (Richter et al. 2001). However, relatively little is known of this region for unsaturated phospholipids. Thus, one intention of this work was to extend the existing partial phase diagram

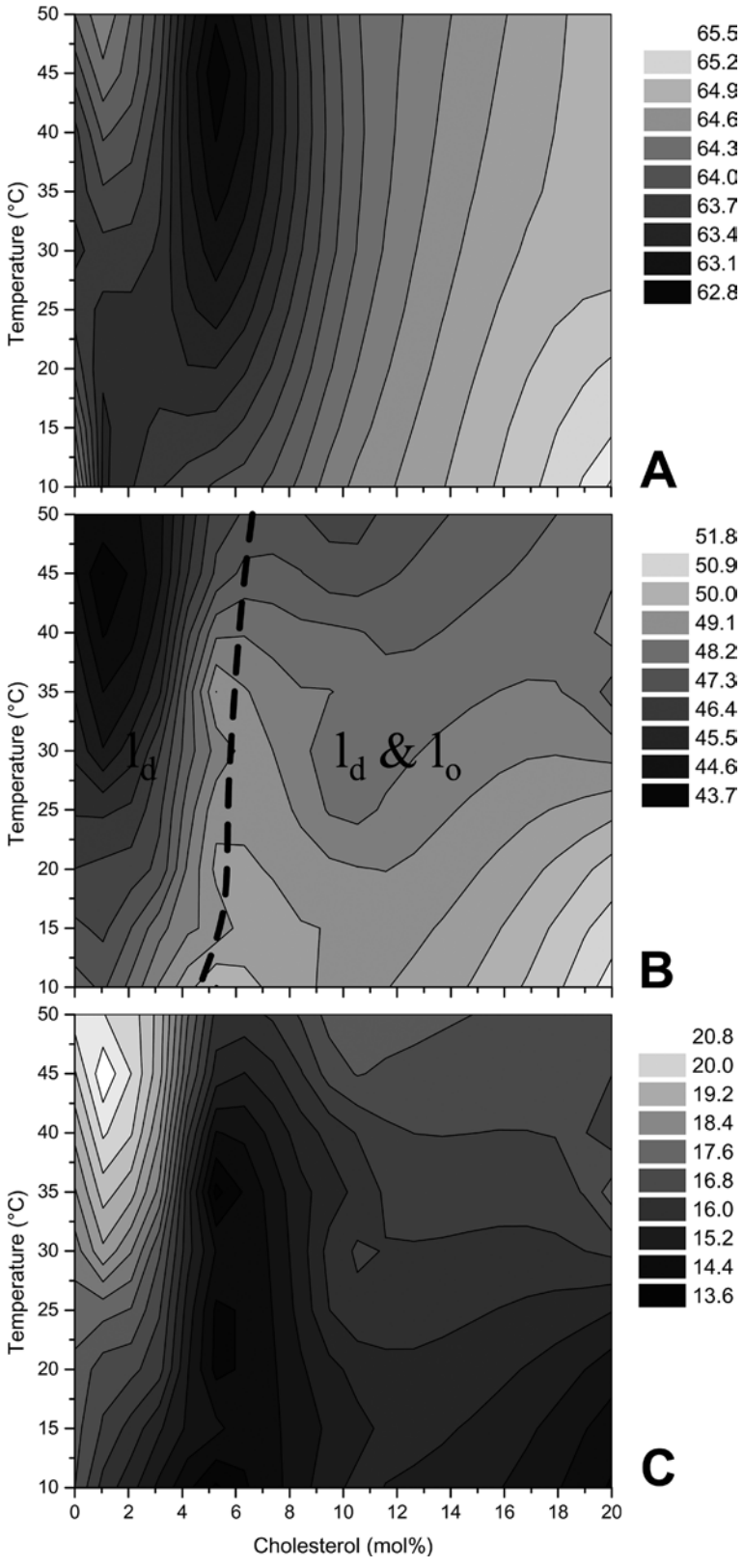

Fig. 6A–C Temperature- and cholesterol-dependent contour maps. **A** *d*-spacing; **B** bilayer spacing d_B; and **C** interbilayer water spacing d_W of POPC. All membrane spacings are given in Å

for POPC (Thewalt and Bloom 1992; Mateo et al. 1995), both in the temperature and pressure directions, and further also to focus on the effect of very low concentrations of cholesterol (< 5 mol%).

First of all, we have examined the *p*-*T*-cholesterol phase diagram for POPC multilamellar liposomes. The slopes for the transition line between the gel and fluid phase boundary dp_m/dT are, in the explored cholesterol

Table 2 Relaxation parameters for POPC at a T-jump amplitude of 3 °C (compare Fig. 7). The relaxation kinetics of the *d*-spacing can be seen as a harmonic one-dimensional overdamped oscillation (Pabst et al. 2000b). From the relaxation constants given in Eq. (1) the frequency ω_0, the damping factor δ, the relaxation velocity v_0, and the relaxation acceleration a_0 at $t = 0$ have been deduced. Δd_{max} is the maximal thinning induced by the T-jump perturbation

	POPC	POPC/1 mol% cholesterol	POPC/5 mol% cholesterol	POPC/10 mol% cholesterol	POPC/25 mol% cholesterol
ω_0 (s^{-1})	0.156 ± 0.007	0.47 ± 0.02	0.58 ± 0.03	0.297 ± 0.009	0.17 ± 0.01
δ (s^{-1})	0.19 ± 0.01	0.81 ± 0.07	1.0 ± 0.1	0.43 ± 0.02	0.28 ± 0.04
v_0 (Å/s)	0.19 ± 0.03	0.61 ± 0.06	1.04 ± 0.25	0.39 ± 0.07	-0.08 ± 0.07
a_0 (Å/s^2)	-0.05 ± 0.01	-0.8 ± 0.3	-1.7 ± 0.6	0.24 ± 0.06	0.05 ± 0.04
Δd_{max} (Å)	-1.04 ± 0.09	-1.1 ± 0.1	-1.32 ± 0.14	-1.18 ± 0.1	-0.38 ± 0.15

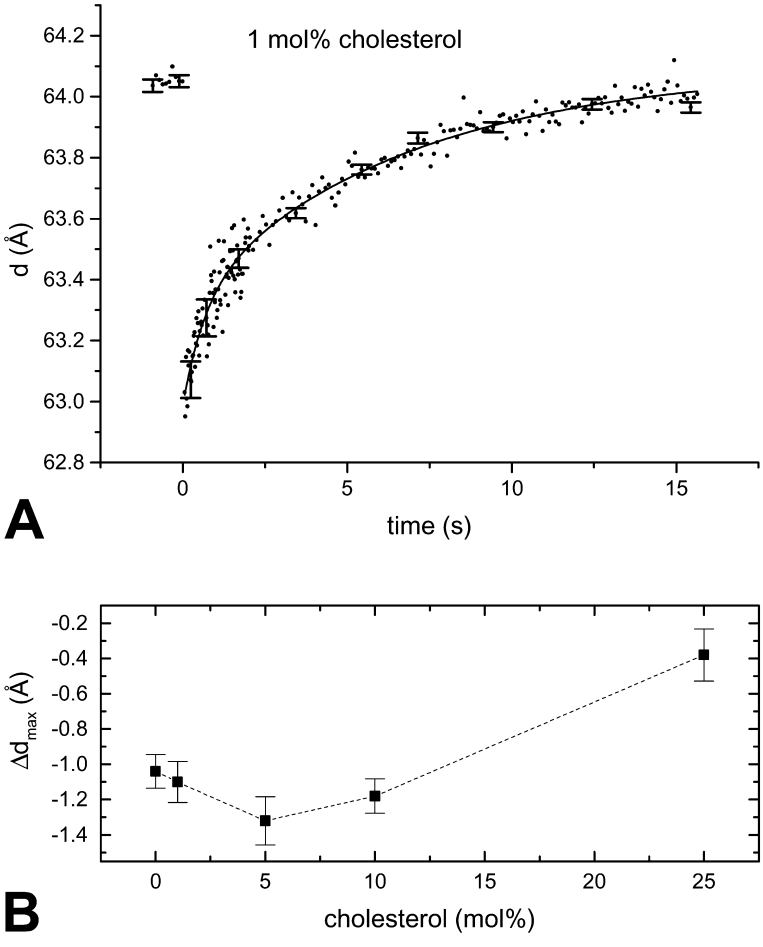

Fig. 7A, B T-jump experiments in the liquid crystalline phase region of POPC. The initial temperature was set to 10 °C and the T-jump amplitude was 3 °C (for detailed results see Table 2). **A** Typical temporal evolution of the lamellar repeat distances during a T-jump experiment of POPC with the addition of 1 mol% cholesterol. **B** Maximum induced thinning of the *d*-spacing as a function of cholesterol content

concentration, always linear within experimental error and vary for 0–20 mol% cholesterol from of 4.5 to 3.4 MPa/°C (Fig. 3A and B). For pure POPC, the value is in good agreement with the published results of Winter and Czeslik (2000) (4.8 MPa/°C). Corresponding to the slight decrease of T_m from –5 °C (0 mol%) to –7 °C (20 mol%) (Thewalt and Bloom 1992), the phase boundary slopes dp_m/dT also decrease slightly. Last, the transition enthalpies decrease from 20 to 7 kJ/mol (Fig. 3C), which compare to values measured by Davis et al. (1981) (pure POPC: $\Delta H_m = 19$ kJ/mol) and Davis and Keough (1983) (SOPC/cholesterol). This decrease in the transition enthalpy can be attributed to a decrease in the cooperativity of the transition. Summarizing, the general phase diagram of the PC/cholesterol mixtures – now also covering the variable of hydrostatic pressure – appears to be universal, including PCs with mono- unsaturated chains. In fact, the slopes for the transition line between the gel and fluid phase boundary in excess of water compare well to the ones of saturated species like DMPC or DPPC (4.5 MPa/°C). Also the freezing point is only slightly reduced by increasing the cholesterol content.

Thus, the most significant difference in the phase diagram as compared to saturated lipids is not found in the phase boundary region between the fluid and gel

phases, but instead is most pronounced in the miscibility gap region. As can be judged from Fig. 6B, the *ld*/*lo* phase boundaries are strongly enlarged as compared to saturated lipids. Even 55 °C above the main transition, still no critical behaviour can be found in the POPC/cholesterol system, which compares, for example, to DMPC with a critical temperature of about 45 °C at 20 mol% cholesterol (Mabrey et al. 1978; Richter et al. 2001). These findings may have biological relevance and will be discussed in more detail below.

The "impurity" regime

Many publications have dealt with the effects of cholesterol at high concentrations, but still little is understood about cholesterol's organization at low concentrations (< 5 mol%) (Laggner et al. 1991; Rukmini et al. 2001). Because there are a number of intracellular organelles, such as the inner mitochondrial membrane, where the cholesterol content is actively maintained at a low level (Bretscher and Munro 1993), any information on cholesterol organization in such membranes will be useful. Lemmich et al. (1997), for instance, have pointed out already that small variations of cholesterol content could provide an effective control of the membrane softness and thereby control the vesicle-budding processes as well as the intermembrane distances in the endoplasmic reticulum and the Golgi apparatus.

The main point for understanding the effect of cholesterol at very low content lies in the molecule's "frustration" neither to pack very well in the solid ordered gel phase nor to like the vicinity of the disordered chains in the fluid phase. In other words, at low concentration, cholesterol is neither able to fully break the crystalline lattice, nor to fully induce order in the acyl chains. Simply, cholesterol may be understood as an "impurity" and due to its non-preference tends to accumulate at defect points, lines or interfaces (Möhwald 1995). Another outcome is that one can identify a narrow two-phase coexistence region of the *ld* and *so* phases around the melting point (Vist and Davis 1990).

Further, in the low-cholesterol regime, an enhancement of density fluctuations was predicted, which in turn implies that response functions, such as specific heat and lateral compressibility, increase especially near the phase transition region (Lemmich et al. 1997). Already very low amounts (< 3 mol%) of cholesterol contribute to the softness of the membrane and thus affect the lipid bilayer fluctuations (Lemmich et al. 1997; Richter et al. 2001). This is in good agreement with our T-jump experiments, where a maximum in the bilayer thinning was measured at 5 mol% (Fig. 7B). Since the T-jump-induced lattice change is directly related to the fluidity of the bilayer system (Pabst et al. 2000b), the results indicate that the membrane is softest at this point. In the low-concentration regime and close to the main phase transition temperature, cholesterol not only softens the bilayer but also increases its permeability (Corvera at al. 1992; Lemmich et al. 1997).

Other findings, such as the progressive increase of the bilayer spacing d_B at the *ld* to *ld*/*lo* phase boundary (see Fig. 6B) or the high sensitivity of the barotropic hysteresis widths even at very low concentrations (e.g., 1 mol%; Fig. 4), support the hypothesis of lateral density fluctuations, especially in the "wings" of the main transition (Cruzeiro-Hansson et al. 1989). In our p-scan experiments, we observe a steady increase of the barotropic hysteresis width up to 5 mol% (Figs. 4 and 5). We attribute this finding for the hysteresis to an increase of the *so*/*ld* coexistence range. This widening in the phase diagram was indeed found experimentally by Vist and Davis (1990), and theoretically simulated by Ipsen et al. (1987), both for DPPC/cholesterol mixtures.

Recently, the role of membrane surface curvature and thickness on the dimer arrangement of cholesterol (< 5 mol%) have been investigated (Rukmini et al. 2001). The formation of such transmembrane dimers was imagined to represent the first step in the ultimate separation of a pure cholesterol domain. However, on the basis of our data, this hypothesis remains speculative, since the detected fluctuations of the bilayer, being equivalent to higher local surface curvature, would suppress its formation.

The miscibility gap

When cholesterol is present at higher concentrations (> 5–8 mol%) it can overcome its "frustration" by inducing a new phase perfectly matching its special, ambivalent character: the liquid but chain-ordered phase *lo*. Its formation is mirrored by our analysis of the bilayer structural properties in the fluid-phase region: up to 3 mol% (e.g., at 10 °C) the lipid bilayer spacing stays quite constant with a value of about 47 Å, and then progressively increases until a new plateau around 49 Å is reached (> 5 mol%; see Fig. 6B). The latter is explained by the massive onset of phase separation and the generation of the *lo* phase, which owing to its ordered chain conformation is known to exhibit a larger bilayer thickness (McIntosh et al. 1989).

In the miscibility gap, where the *ld* and *lo* phases coexist, another important fact can be concluded from our data. The mechanical strength of the membrane increases with the growing fraction of the *lo* phase. Indeed, our T-jump experiments reveal a strong reduction in bilayer compressibility above 5 mol% (Fig. 7B). However, most significant is the relative enlargement of the *ld*/*lo* phase region for POPC as an example for mono-unsaturated lipids. While at physiological temperatures the coexistence range in DMPC spans a concentration interval from about 7 to 28 mol%, in POPC the *ld* phase is conserved even up to a concentration of at least 40 mol% (Mateo et al. 1995). As stated earlier, the miscibility gap is also strongly enlarged in the temperature axis. In Fig. 6B, the difference in bilayer thickness of the *ld* phase with respect to the *ld*/*lo* phase region is

clearly seen even at 50 °C, and thus no critical behaviour can be inferred. This is further confirmed by the X-ray diffraction pattern: POPC and cholesterol form only one lamellar phase, as one can expect for the miscibility gap. In contrast, above the gap, two lamellar phases with different lattice parameters should form (Richter et al. 2001). The fact that the miscibility gap is conserved over a wider concentration and temperature range in unsaturated lipids is explained by the less favourable cross-relaxation rates between cholesterol and the *cis*-bonded chains (Huster and Gawrisch 2000). It might seem plausible that cholesterol shows a preference for the interaction with saturated chains, but the resulting non-randomness of lipid mixtures may have some biological relevance. Only recently, the degree of fatty acid unsaturation was considered to play an important role in the separation of lipid species in this biologically relevant phase region (Mitchell and Litman 1998), where the differential miscibility has been speculated as being the basis for the formation of functional "lipid rafts".

Conclusion

We have performed static, slow and rapid time-resolved X-ray diffraction experiments on the POPC/cholesterol mixtures in multilamellar vesicles by varying temperature, pressure and composition. Our work was focused on the three coexistence regions of the pressure-temperature-cholesterol phase diagram, which are of particular interest for understanding the regulatory function of cholesterol in nature, especially in the presence of unsaturated lipid species.

1. Slow p-scans have demonstrated that the coexistence region between the gel phase (*so*) and the liquid disordered phase (*ld*) increases up to a concentration of 5 mol%.
2. Between 5 and 25 mol%, the *so* and *ld* phases do not mix any more, which reduces the main transition widths. The formation of a new fluid ordered phase *lo* – coexisting both with the *ld* and *so* phase – opposes the latter effect.
3. Rapid temperature perturbations in the *ld* as well as *ld*/*lo* phase regions have confirmed the mechanical properties of the bilayer: up to 5–8 mol%, cholesterol causes a fluidization of the membrane, and above that amount a stiffening is induced, which coincides with the creation of the cholesterol-rich fluid, but chain-ordered phase *lo*. Most noteworthy, the coexistence region of *lo* and *ld* is strongly enlarged for the mono-unsaturated lecithin POPC with respect to saturated PCs, i.e. the *ld* phase is conserved over a broader cholesterol and temperature range. Once more, this underlines the important regulatory role of unsaturated lipids in this regime. Future systematic studies will have to concentrate on the interplay of different lipid mixtures with cholesterol to further test the hypothesis of highly organized and cholesterol-rich complexes, which may provide a nucleation point for important biological processes (Brzustowicz et al. 2002).

References

Almeida PFF, Vaz WLC, Thompson TE (1992) Lateral diffusion in the liquid phases of dimyristoylphosphatidylcholine/cholesterol lipid bilayers: a free volume analysis. Biochemistry 31:6739–6747

Amenitsch H, Rappolt M, Kriechbaum M, Mio H, Laggner P, Bernstorff S (1998) First performance assessment of the SAXS beamline at ELETTRA. J Synchrotron Radiat 5:506–508

Anderson TG, McConnell HM (2001) Condensed complexes and the calorimetry of cholesterol-phospholipid bilayers. Biophys J 81:2774–2785

Bernstorff S, Amenitsch H, Laggner P (1998) High-throughput asymmetric double-crystal monochromator for the SAXS beamline at ELETTRA. J Synchrotron Radiat 5:1215–1221

Bloch K (1965) The biological synthesis of cholesterol. Science 150:19–28

Bloch K (1983) Sterol structure and membrane function. CRC Crit Rev Biochem 14:47–92

Bloch K (1994) Blonds in Venetian paintings, the nine banded armadillo, and other essays in biochemistry. Yale University Press, New Haven

Bloom ME, Mouritsen OG (1995) The evolution of membranes. In: Lipowsky R, Sackmann E (eds) Handbook of biological physics, vol 1. Elsevier, Amsterdam, pp 65–95

Bretscher MS, Munro S (1993) Cholesterol and the Golgi apparatus. Science 61:1280–1281

Brzustowicz MR, Cherezov V, Caffrey M, Stillwell W, Wassall SR (2002) Molecular organization of cholesterol in polyunsaturated membranes: microdomain formation. Biophys J 82:285–298

Chiu SW, Jakobson E, Scott HL (2001) Combined Monte Carlo and molecular dynamics simulation of hydrated lipid-cholesterol at low cholesterol concentration. Biophys J 80:1104–1114

Corvera E, Mouritsen OG, Singer MA, Zuckermann MJ (1992) The permeability and the effect of acyl chain length for phospholipid bilayers containing cholesterol: theory and experiment. Biochim Biophys Acta 1107:261–270

Cruzeiro-Hanson L, Ipsen JH, Mouritsen OG (1989) Intrinsic molecules in lipid membranes change the lipid-domain interfacial area: cholesterol at domain interfaces. Biochim Biophys Acta 979:166–176

Davis PJ, Keough KMW (1983) Differential scanning calorimetry studies of aqueous dispersions of mixtures of cholesterol with some mixed-acid and single-acid phosphatidylcholines. Biochemistry 22:6334–6340

Davis PJ, Fleming BD, Coolbear KP, Keough KMW (1981) Gel to liquid-crystalline transition temperatures of water dispersions of two pairs of positional isomers of unsaturated mixed-acid. Biochemistry 20:3633–3636

Dietrich C, Bagatolli LA, Volovyk ZN, Thompson NL, Levi M, Jakobson K, Gratton E (2001) Lipid rafts reconstituted in model membranes. Biophys J 80:1417–1428

Drake CM, Burton JL (1998) Effect of cholesterol on molecular order and dynamics in highly polyunsaturated phospholipid bilayers. Biophys J 75:896–908

Finegold L (1993) Cholesterol in membrane models. CRC Press, Boca Raton

Huang TC, Toraya H, Blanton TN, Wu YJ (1993) X-ray powder diffraction of silver behenate, a possible low-angle diffraction standard. J Appl Crystallogr 26:180–184

Huster D, Gawrisch K (2000) New insights into biomembrane structure from two-dimensional nuclear Overhauser enhancement spectroscopy. In: Katsaras J, Gutberlet T (eds) Lipid bilayers. Structure and interactions. Springer, Berlin Heidelberg New York, pp 109–125

Ichimori H, Hata T, Matsuki H, Kaneshina S (1999) Effect of unsaturated acyl chains on the thermotropic and barotropic

phase transitions of phospholpid bilayer membranes. Chem Phys Lipids 100:151–164
Ipsen JH, Karlström G, Mouritsen OG, Wennerström H, Zuckermann MJ (1987) Phase equilibria in the phosphatidylcholine-cholesterol system. Biochim Biophys Acta 905:162–172
Ipsen JH, Mouritsen OG, Bloom M (1990) Relationships between lipid membrane area, hydrophobic thickness, and acyl-chain orientational order. The effects of cholesterol. Biophys J 57:405–412
Jamieson GA, Robinson DM (1977) Mammalian cell membranes, vol 2. Butterworth, London
Kriechbaum M, Laggner P, Rapp G (1990) Fast time-resolved X-ray diffraction for studying laser T-jump-induced phase transitions. Nucl Instr Methods A 291:41–45
Laggner P, Lohner K, Koynova R, Tenchov B (1991) The influence of low amounts of cholesterol on the interdigitated gel phase of hydrated dihexadecylphosphatidylcholine. Chem Phys Lipids 60:153–161
Laggner P, Amenitsch H, Kriechbaum M, Pabst G, Rappolt M (1999) Trapping of short lived intermediates in phospholipid phase transitions: the L_α* phase. Faraday Discuss 111:31–40
Lange Y, Ye J, Rigney M, Stack TL (1999) Regulation of ER cholesterol by plasma membrane cholesterol. J Lipid Res 40:2264–2270
Lemmich J, Mortensen K, Ipsen JH, Hønger T, Bauer R, Mouritsen OG (1997) The effect of cholesterol in small amounts on lipid-bilayer softness in the region of the main phase transition. Eur Biophys J 25:293–304
Mabrey S, Mateo PL, Sturtevant JM (1978) High-sensitivity scanning calorimetric study of mixtures of cholesterol with dimyristoyl- and dipalmitoylphosphatidylcholines. Biochemistry 17:1464–2468
Mateo CR, Acuña AU, Brochon J-C (1995) Liquid-crystalline phases of cholesterol/lipid bilayers as revelead by the fluorescence of *trans*-parinaric acid. Biophys J 68:978–987
McIntosh, TJ, Magid AD, Simon SA (1989) Cholesterol modifies the short-range repulsive interactions between phosphatidylcholine membranes. Biochemistry 28:17–25
McMullen TPW, McElhaney RN (1995) New aspects of the interaction of cholesterol with dipalmitoylphosphatidylcholine bilayers as revealed by high-sensitivity differential scanning calorimetry. Biochim Biophys Acta 1234:90–98
McMullen TPW, Ruthven NAH, McElhaney RN (1993) Differential scanning calorimetric study of the effect of cholesterol on the thermotropic phase behavior of a homologous series of linear saturated phosphatidylcholines. Biochemistry 32:516–522
Melchior DL, Scavitto FJ, Steim JM (1980) Dilatometry of dipalmitoyllecithin-cholesterol bilayers. Biochemistry 19:4828–4834
Miao L, Nielsen M, Thewalt J, Ipsen JH, Bloom M, Zuckermann MJ, Mouritsen OG (2002) From lanosterol to cholesterol: structural evolution and differential effects on lipid bilayers. Biophys J 82:1429–1444
Mitchell DC, Litman BJ (1998) Effect of cholesterol on molecular order and dynamics in highly polyunsaturated phospholipid bilayers. Biophys J 75:896–908
Möhwald H (1995) Phospholipid monolayers. In: Lipowsky R, Sackmann E (eds) Handbook of biological physics, vol 1. Elsevier, Amsterdam, pp 161–211
Mouritsen OG, Jørgensen K (1994) Dynamical order and disorder in lipid bilayers. Chem Phys Lipids 73:3–25
Nielsen M, Miao L, Ipsen JH, Zuckermann MJ, Mouritsen OG (1999) Off-lattice model for the phase behavior of lipid-cholesterol bilayers. Phys Rev E 59:5790–5803
Pabst G, Rappolt M, Amenitsch H, Laggner P (2000a) Structural information from multilamellar liposomes at full hydration: full *q*-range fitting with high quality X-ray data. Phys Rev E 62:4000–4009
Pabst G, Rappolt M, Amenitsch H, Bernstoff S, Laggner P (2000b) X-ray kinematography of temperature-jump relaxation probes the elastic properties of fluid bilayers. Langmuir 16: 8994–9001
Parasassi T, Giusti AM, Raimondi M, Gratton E (1995) Abrupt modifications of phospholipid bilayer properties at critical cholesterol concentrations. Biophys J 68:1895–1902
Pasenkiewicz-Gierula M, Subczynski WK, Kusumi A (1990) Rotational diffusion of steroid molecule in phosphatidylcholine-cholesterol membranes: fluid phase microimmiscibility in unsaturated phosphatidylcholine-cholesterol membranes. Biochemistry 20:4505–4510
Pressl K, Kriechbaum M, Steinhart M, Laggner P (1997) High pressure cell for small- and wide-angle X-ray scattering. Rev Sci Instrum 68:4588–4592
Presti FT (1985) The role of cholesterol in membrane fluidity. In: Aloia RC, Boggs JM (eds) Membrane fluidity in biology, vol 4. Academic Press, New York, pp 97–146
Radhakrisnan A, McConnell HM (1999) Condensed complexes of cholesterol and phospholipid. Biophys J 77:1507–1517
Rapp G, Goody RS (1991) Light as a trigger for time-resolved structural experiments on muscle, lipids, p21 and bacteriorhodopsin. J Appl Crystallogr 24:857–865
Richter F, Rapp G, Finegold L (2001) Miscibility gap in fluid dimyristoylphosphatidyl-choline:cholesterol as "seen" by X-rays. Phys Rev E 63:051914–051924
Rukmini R, Rawat SS, Biswas SC, Chattapadhyay A (2001) Cholesterol organization in membranes at low concentrations: effects of curvature stress and membrane thickness. Biophys J 81:2122–2134
Sankaram MB, Thompson TE (1991) Cholesterol-induced fluid-phase immiscibility in membranes. Proc Natl Acad Sci USA 88:8686–8690
Salem N Jr (1989) Fatty acids: molecular and biochemical aspects. In: Spiller GA, Scala J (eds) New protective roles for selected nutrients. Liss, New York, pp 109–228
Scott HL (1993) Lipid-cholesterol phase diagrams: theoretical and numerical aspects. In: Finegold L (ed) Cholesterol in membrane models. CRC Press, Boca Raton, pp 197–221
Smaby JM, Momsen MM, Brockmann HL, Brown RE (1997) Phosphatidylcholine acyl unsaturation modulates the decrease in interfacial elasticity induced by cholesterol. Biophys J 73:1492–1505
Steinhart M, Kriechbaum M, Pressl K, Amenitsch H, Bernstorff S, Laggner P (1999) High-pressure instrument for small- and wide-angle X-ray scattering II. Time-resolved experiments. Rev Sci Instrum 70:1540–1545
Thewalt JL, Bloom M (1992) Phosphatidylcholine: cholesterol phase diagrams. Biophys J 63:1176–1181
Tu K, Klein ML, Tobias DJ (1998) Constant-pressure molecular dynamics investigation of cholesterol effects in a dipalmitoylphosphatidylcholine bilayer. Biophys J 75:2147–2156
Vist MR, Davis JH (1990) Phase equilibria of cholesterol/dipalmitoylphosphatidylcholine mixtures: ^{2}H nuclear magnetic resonance and differential scanning calorimetry. Biochemistry 29:451–464
Winter R, Pilgrim W-C (1989) A SANS study of high pressure phase transition in model biomembranes. Ber Bunsenges Phys Chem 93:708–717
Winter R, Czeslik C (2000) Pressure effects on the structure of lyotropic lipid mesophases and model biomembrane systems. Z Kristallogr 215:454–474
Worthman LA, Nag K, Davis PJ, Keough KM (1997) Cholesterol in condensed and fluid phosphatidylcholine monolayers studied by epifluorescence microscopy. Biophys J 72:2569–2580
Yeagle PL (1993) The biophysics and the cell biology of cholesterol: an hypothesis for the essential role of cholesterol in mammalian cells. In: Finegold L (ed) Cholesterol in membrane models. CRC Press, Boca Raton, pp 1–12